Elastic Characterization of Porous Bone by Ultrasonic Method through Lamb Waves

Lahcen Mountassir *, Touriya Bassidi, Hassan Nounah

Laboratory of Metrology and Information Processing, Faculty of Science, Ibn Zohr University, Agadir, Morocco

ARTICLE INFO

Article history:

Received 18 October 2016
Accepted 23 January 2017
Available online 25 June 2017

Keywords:

Bone
Porous materials
Elastic properties
Lamb waves
Ultrasound

ABSTRACT

The aim of this research is to characterize the porous bones by an ultrasonic method using Lamb waves. In recent years, characterization of such materials has attracted much attention of the researchers in the field of medicine. It requires the development of more efficient technology for obtaining the necessary quality and security. This paper aims to exploit the dispersion curves of the Lamb wave, as a new originate alternative, to characterize the porous bone. The method is modeled by using the Schoch theory for the measurement of ultrasonic parameters, namely the longitudinal and transversal velocities and densities, and then we deduce the mechanical properties of samples with different porosity in a theoretical way. The theoretical results were compared with experimental data, and it was found that the predicted values were of the same order of measurement as the experimental ones. The correlation coefficient between the experimental ultrasound velocities and the theoretical velocities predicted by the Schoch theory was R=0.96.

1-Introduction

The use of acoustic phenomena (including ultrasonic) to characterize bone tissue should diagnose osteoporosis with high reliability and to effect a monitoring of the evolution of the disease, especially during its processing [1]. Before this can happen, extensive research should be carried out to understand how to set the vibration and acoustic fields in the bone tissue, and how to extract the bones characteristic parameters in these areas. In recent years, Lamb waves have been a great interest [2–7] as a vehicle for in-vivo diagnosis of osteoporosis and other bone afflictions [8].

The ultrasonic technique is more suitable to be used in medicine [9]. The elastic wave velocity in the bone depends on the following parameters: density, porosity, saturated fluid and temperature [10-11]. This study aims to correlate the elastic wave velocities with the mechanical properties of the bone. Furthermore, the primary objective of this paper is to use the dispersion curves as a new original alternative for characterizing porous materials in general and porous bones in particular. We brought the propagation of Lamb waves, in particular, according to the porosity of cancellous bone. This unusual phenomenon is considered to become a powerful tool for the diagnosis of osteoporosis because the wave propagation behavior is apparently dependent on the bone structure.

Accordingly, some studies have been published for the diagnosis of osteoporosis, i.e. monophotonic absorptiometry, biphotonic absorptiometry, two-energy X-ray

* Corresponding author:
E-mail address: mountassir.lahcen8@gmail.com

absorptiometry (DEXA), and quantitative computed tomography [12]. The main advantage of using the ultrasonic wave propagation in porous bone is that it is a non-destructive and non-invasive technique [10-11], providing information on the sample in the vicinity of the solid-liquid interfaces.

The first part of this article presents a modeling study to determine the mechanical properties of the porous bones depending on the porosity degree using the Schoch model. This model is used for modeling the Lamb wave propagation in the porous bone. In the second part of this paper, we carry out an experimental study by an ultrasound method to define the mechanical properties of the porous bone according to the porosity ratio. The innovative part is devoted to the study of the possibility of replacing the regular destructive testing by ultrasonic non-destructive techniques to determine the physical and mechanical properties of porous materials [10-11]. To do this, we must develop an ultrasonic transmission method in which the sample is emerged in water. We used two identical plan transducers with 5MHz in the center frequency. So, we prepared the sample of bovine trabecular bone as well polished bony plates.

2-Materials and Methods

2-1-Theoretical study

2-1-1- Schoch theory

In recent years, a theoretical simulation of power reflector Schoch has been developed [13, 14]. This simulation allows calculating the reflection coefficient at the interface between the coupling liquid and homogeneous, semi-infinite materials [15–17]. The input parameters are the velocity of the acoustic wave in the coupling liquid V_{liq}, the velocities of the longitudinal and transversal modes in the studied material, V_l and V_t, and the density of the liquid and the solid, ρ_l and ρ_t.

To introduce the porosity of the porous materials it is necessary to make changes in the acoustic parameters. Phani and Maitra [18, 19] proposed an expression for the longitudinal velocity of porous materials that take into account the morphology of the pore and are valid for all porosity values to solve this problem. This empirical relationship is formulated as:

$$V_l = V_{l0}(1-\varphi)^p \quad (1)$$

where V_l is the bone longitudinal wave velocity, φ is the bone porosity, V_{l0} is the bone longitudinal for $\varphi = 0$, and $\boldsymbol{p}$ constant coefficient depends on the pore morphology.

The Phani equation is modified when working in a porous medium saturated with a fluid. This equation must take into account the saturating fluid velocity, V_f. In this case, we have the relation:

$$V_l = V_{l0}(1-\varphi)^m + \varphi V_f \quad (2)$$

We know that transverse waves do not propagate in fluids; that is why we selected an empirical relationship for the transverse velocity approximating that given by expression (1):

$$V_t = V_{t0}(1-\varphi)^s \quad (3)$$

where V_t is the bone transversal wave velocity, V_{t0} is the bone transversal velocity for $\varphi = 0$.

The dependence of the parameters m and s with the geometry of the pores in the porous media has been studied by Phani [18, 19]. He found that the values of these numbers ranged between 0.5 and 1.5 for a relatively ordered porous structure. For cylindrical pores, ***m*** and ***s*** are close to one, and for spherical pores the values get closer to 0.5. In this study we considered cylindrical pores ***m=s=1***.

The granny ways relies on densities of the non-porous part ρ_s, the fluid portion ρ_f and the porosity φ of the porous medium by the following expression:

$$\rho_p = \rho_s(1-\varphi) + \varphi\,\rho_f \quad (4)$$

The Victorov relationship [20] could easily determine the velocity of Rayleigh waves, V_R using longitudinal and shear velocities:

$$V_R = V_t \frac{0.718 - (V_t/V_l)^2}{0.750 - (V_t/V_l)^2} \quad (5)$$

In the following paragraphs, we will present numerical simulation results obtained from the Schoch theory for Lamb wave propagation when

considering a homogeneous and non-porous medium corresponding to porous medium acoustic characteristics.

2-1-2- Modeling of Lamb waves in porous bones

2-1-2-1- Lamb modes

The plate model has been used by many researchers for modeling the propagation of elastic waves in the porous bone [10, 15, 21–25]. The wave propagation in elastic plates gives rise, in general, to guided waves known as Lamb waves. Many studies conducted by various researchers suggest that under certain conditions, the trabecular bone plate behaves as a waveguide. Some researchers have also extended the wave propagation model in the trabecular bone to the distribution model in the plates.

Lamb waves exist in the form of resonance modes or frequency and phase velocity resulting in a standing wave between the boundaries of the plate. The longitudinal and transversal components give rise to symmetrical and anti-symmetrical modes (Fig. 1). The symmetric modes are longitudinal modes or compression modes which are rated as S_n with $n \geq 0$. The anti-symmetrical modes are bending modes which are estimated A_n with $n \geq 0$ [24].

To study the different modes which are generated in a homogeneous and isotropic plate, one has to resolve the problem of propagation of elastic waves in a plate placed in the void [25]. The solutions of the equation about the wave propagating at the plate have to satisfy the boundary conditions, and this leads to the dispersion equations of the symmetric (S) and anti-symmetric (A) Lamb modes (Fig. 2) [24].

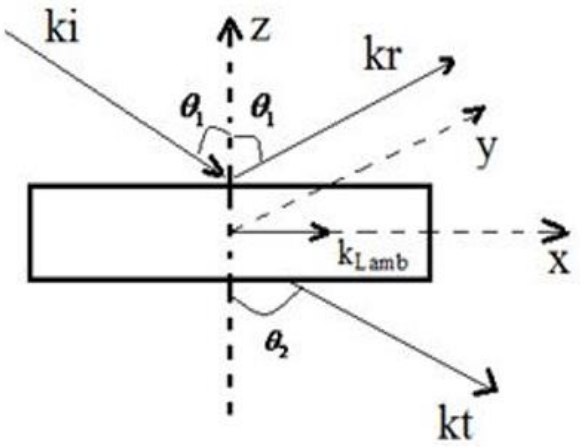

Fig. 1. Geometry problem [25].

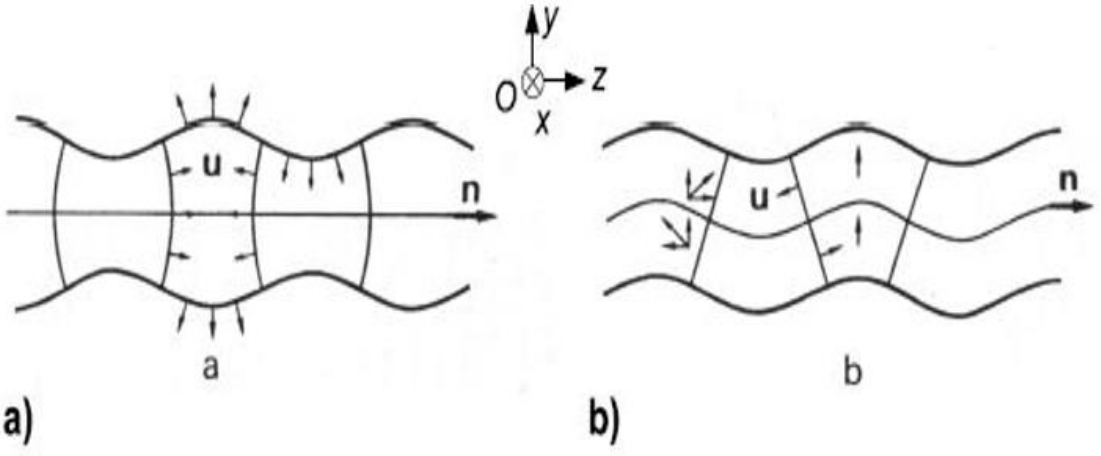

Fig 2. Strain in an isotropic plate due to the propagation of Lamb waves corresponding to a mode: a) symmetric, b) anti-symmetric. The vector n is the direction of propagation; the vector u is the displacement vector [26].

2-1-2-2- Reflection and transmission coefficients

Some theoretical and experimental studies have shown that the reflection coefficient (transmission respectively) has singularities when a surface wave (Rayleigh wave) or a guided wave (Lamb wave) is energized.

These phenomena have been studied from the analytical expression of the reflection coefficient of a plane wave by an infinite fluid-solid interface semi-infinite, and fluid- fluid interface. These studies provide the one hand interpretation of the singularities of the reflection coefficients (transmission respectively) regarding the excitation of guided or surface waves and, on the contrary, show the similarities between the type of guided Lamb waves and Rayleigh surface waves [24-26].

The reflection coefficient (R) and transmission coefficient (T) of a plan incident wave at an incident angle θ, by an immersed plate, may be placed into the form [26]:

$$R = \frac{C_a C_s - \tau^2}{(C_a + j\tau)(C_s - j\tau)} \quad (6)$$

$$T = j\tau\left(\frac{1}{(C_a + j\tau)} + \frac{1}{(C_s - j\tau)}\right) \quad (7)$$

with $\tau = \frac{Z_1}{Z_L}$ Or Z_1 is the acoustic impedance of the water and Z_L is the longitudinal acoustic impedance of the material under study. C_a and C_s are linked to anti-symmetric and symmetric deformations of faces, respectively. The terms C_a and C_s are from the continuity conditions of displacements and efforts to plate/water interfaces. They are given by the following expressions [26]:

$$C_a = cos^2(2\gamma) tan\frac{P}{2} + \left(\frac{V_T}{V_L}\right)^2 \sin(2\theta)\sin(2\gamma)\, tan\frac{Q}{2} \quad (8)$$

$$C_s = cos^2(2\gamma) cot\frac{P}{2} + \left(\frac{V_T}{V_L}\right)^2 \sin(2\theta)\sin(2\gamma)\, cot\frac{Q}{2} \quad (9)$$

where $Q = k_T \cos(\gamma)\, d$ and $P = k_L \cos(\theta)\, d$

Assuming that guided waves are generated in the plate, Schoch [13] showed that equations (8) and (9) give the natural frequencies of the vibration modes of a immersed plate in water. They correspond to the poles of the transmittance (reflection respectively) given in the previous paragraph.

$$C_a + j\tau = 0\,, \quad C_s - j\tau = 0 \quad (10)$$

The last equations are actually Rayleigh-Lamb equations for an immersed plate the direction of propagation, and vector u is the displacement vector [26]. If the fluid has a much lower density compared with the solid, the poles of the reflection coefficients correspond to the excitation of an anti-symmetric Lamb mode ($C_a = 0$) or symmetric ($C_s = 0$). In summary, the excitation of an anti-symmetrical Lamb mode or symmetrical modes manifests itself by a maximum of the transmission coefficient (cancellation of the reflection coefficient), and vice versa. Observing a maximum transmittance (zero in reflection coefficient) to a frequency and a given incident angle reflects the existence of a Lamb mode propagating at this frequency in the plate.

In this paragraph, the equations of a self-dispersion plate and an immersed plate were established. The influence of the existence of Lamb waves on the reflection and transmission coefficients was emphasized. According to the theoretical exposition, the excitement of a Lamb mode by the incident beam is reflected by the maximum transmission rate (minimum reflection coefficient). The dispersion curves of a plate immersed in a fluid are then obtained by finding the maxima of the transmission coefficient.

2-2- Experimental study

2-2-1- Specimen preparation

A series of innovative measures were carried out on bovine bone samples. The heads of the femoral bone were used to cut these samples in parallelepiped form. They are of varying thicknesses and densities. At first rough cut was performed to eliminate the cortical layer and uncover the trabecular bone alone. Then, a much finer cut was performed using a diamond saw to low speed rotating. Distilled water was used to

lubricate and cool the saw in the second process to avoid damaging the surface of the specimen cut [27]. The samples were immersed in hot water to remove the soft tissues and the bone marrow residues contained in the pores. They were then washed under high pressure with cold water. After repeating the operation several times, the samples were first immersed for 24 hours in distilled water and then stored in a solution of trichlorethylene for four hours and washed again in distilled water bath for 24 hours.

2-2-2- Experimental setup

Fig. 6 shows the experimental setup of ultrasound measurements used in this study. The transducer and the samples are immersed in water. The sensors with a central frequency of 5MHz transmit longitudinal ultrasonic waves to the bone through the water after it receives the ultrasound waves through the sample. The emitter transducer is excited using an ultrasonic pulse generator which also plays the role of an amplifier of the sensed signals. The generator is connected to a PicoScope to acquire the signal through the sample. The signals picked up with the PicoScope are recovered on a computer. The signs revealed on the computer using a Pico-Scope National Instrument. The LabView software examines PicoScope, so we have developed a platform in the favorable environment of the software to process ultrasound signals acquired to deduce the ultrasonic parameters of the trabecular bone.

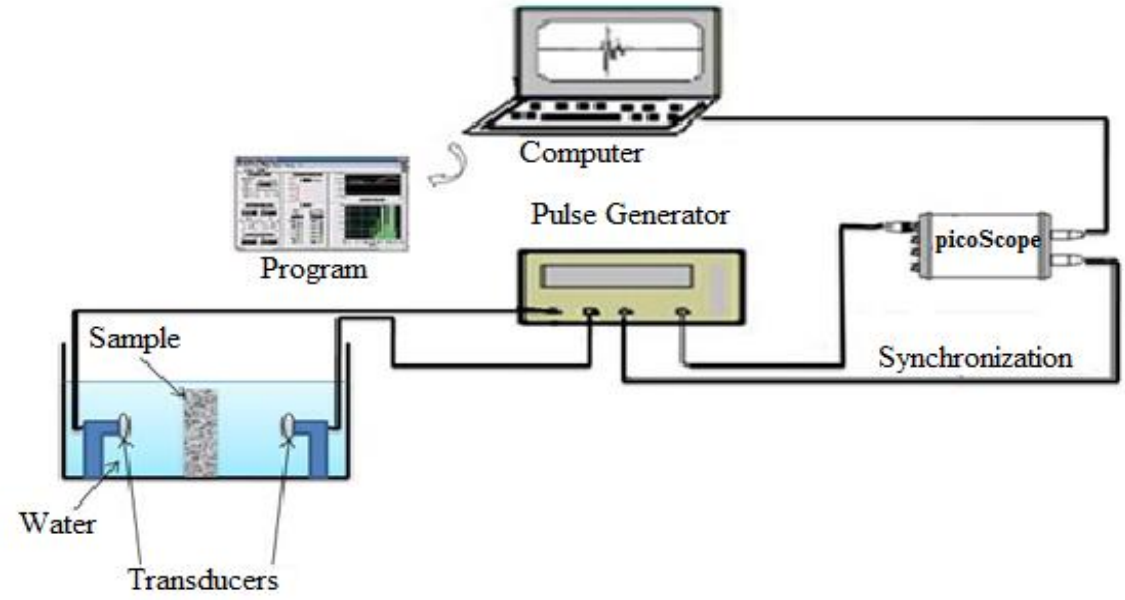

Fig. 3. Schematic diagram of the apparatus used in the experiments.

3- Results and Discussion

3-1- Numerical simulation of dispersion curves

The method employed in this study consists of seeking maxima of the transmittance modulus of a plate immersed in a fluid (water in this case). These peaks correspond to the Lamb waves. The model developed allows, therefore, for an angular and frequency scanning determining the pairs (incidence angle, frequency) for which a Lamb wave propagates by [26]: $\frac{\rho_{fluid}}{\rho_{plate}} \ll 0$.

Moreover, the program for this prediction is executed using Matlab. The acoustic parameters of the materials (bone, water, and air) used in this calculation are shown in Table1. Fig. 3 presents the theoretical dispersion curves of the steel plate of 2 mm thick. This figure shows the different modes and areas of critical angles. It should be noted that the curves of the higher order modes all undergo an infection around the critical angle of the longitudinal waves θ_{cl} to converge towards the critical angle of the transverse waves θ_{ct} in the material. The zero-order modes converge at high frequency to the critical angle of Rayleigh θ_{cR}.

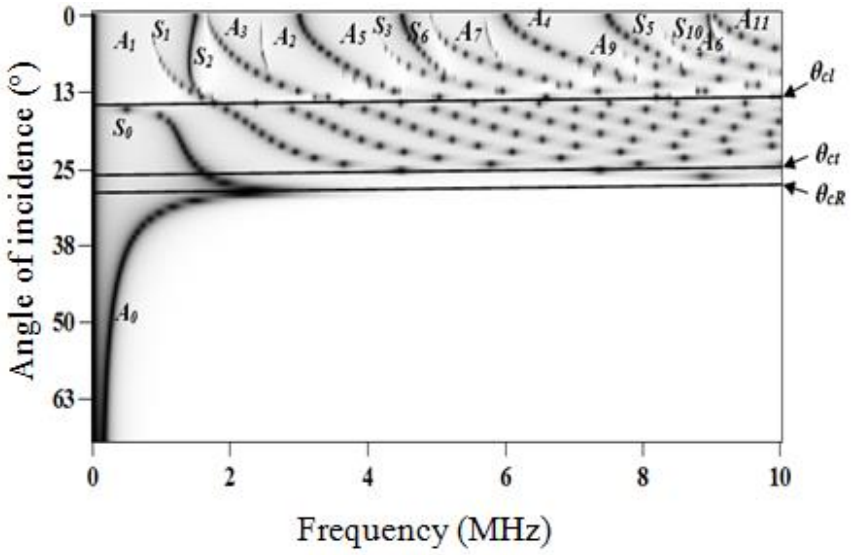

Fig. 4. The theoretical dispersion curves of the steel plate of 2 mm thick.

Table 1. Acoustic properties of trabecular bone, water, and air [9].

	Density (kg/m^3)	**Longitudinal velocity** *(m/s)*	**Transversal velocity** *(m/s)*
Trabecular bone	1960	3861	1981
Water	1000	1500	-
Air	1	300	-

Figs. 4 and 5 show the Lambs waves dispersion curve of the studied bone plates for the air-saturated and water-saturated bone, respectively. For each porosity bone, we represent the corresponding dispersion curve. From the dispersion curves of the air-saturated bone and that of water-saturated bone, we can compare the effect of water and air as saturation fluid on the propagation of ultrasonic Lamb waves. From Figs. 4 and 5 we have observed that the more the porosity increases the higher the critical angles will be. Therefore, under the law of Snell-Descartes [15], the velocities of longitudinal and transversal sound wave are becoming smaller.

We note that the dispersion curves differ from a plate to another depending on the porosity degree. This difference is related to the number of modes, the frequency of occurrence, and the frequency band between two continuous modes. These curves clearly show the dispersive and multimodal nature of the Lamb wave propagation in each plate. Also, they confirm the smooth running of the algorithm created as part of this work.

By analyzing these acoustic signatures along the axis angles or frequencies, we can draw significant findings.

Interpretation of these acoustic signatures along the angles axis highlights the existence of two areas of analysis: for example, in the case of porosity equal to 10% the first extends to about 28° which corresponds to the critical angle for the longitudinal wave propagation. The second critical angle to about 50° corresponds to the critical angle of the transverse wave propagation. Note that the curves of higher order modes suffer any infection around the critical angle of longitudinal waves to converge to the critical angle of transverse waves in the material. It should be noted that there are two areas of analysis following the frequency axis: the first is extended up to about 3MHz. The region where there is only the fundamental Lamb mode: A_0 and S_0. The second is extended from 3 to 5 MHz where the modes are highly dispersive. In this

region, there are the higher order propagation modes of different types of the wave.

Another interesting aspect of these curves concerns their convergence at high frequencies. When the frequency tends to infinity, the fundamental modes A_0 and S_0 converge to the velocity of the Rayleigh mode in the material (little less than the transversal velocity), while the order modes curves above all suffer a bend about the longitudinal velocity to converge to the transversal velocity of the material (See Fig. 4-a for a porosity of bone $\varphi = 5\%$). Whereas when the frequency becomes large, the fundamental modes A_0 and S_0 tend towards a limit angle value. This value allows obtaining the Rayleigh velocity in the material [27]. On the other hand, low frequency, mode S_0, approaches a constant value corresponding to the critical angle of longitudinal waves, and its dispersion is minimal, while mode A_0 decreases monotonically to zero, with maximum dispersion. To prove the distribution of different wave velocities according to the porosity degree in the systems studied, it is necessary to calculate the wave velocities (longitudinal, transversal and Rayleigh) at various porosity rates.

It should be noted that we can exploit the dispersion curves obtained theoretically to measure the longitudinal (V_L), transversal (V_T), and Rayleigh (V_R) velocities in the bone plates. Knowing the critical angles of longitudinal (θ_{cL}), transverse (θ_{cT}), and Rayleigh (θ_{cR}) waves, we deduce speeds, using the following formulas:

$$V_L = \frac{V_{water}}{\sin(\theta_{cL})}$$
$$V_T = \frac{V_{water}}{\sin(\theta_{cT})}$$
$$V_R = \frac{V_{water}}{\sin(\theta_{cR})} \quad (11)$$

From these results, we could highlight the different wave velocities (longitudinal, transverse and Rayleigh) versus porosity rate to arrive at calculating the evolution of various elastic parameters depending on the porosity of the bone plate.

After measurement of speeds, we can recover the mechanical properties of porous bone; we automatically go back to the mechanical properties by using the following theoretical relations:

$$E = \rho V_t^2 \left(\frac{3V_l^2 - 4V_t^2}{V_l^2 - V_t^2} \right) \quad (12)$$

$$\nu = \frac{\frac{1}{2}\left(V_t/V_l\right)^2 - 1}{\left(V_t/V_l\right)^2 - 1} \quad (13)$$

$$G = \frac{E}{2(1+\nu)} \quad (14)$$

Where E, G and ν are Young's modulus, transverse module, and Poisson ratio, respectively.

Table 2 shows the simulation results of our theoretical measures, namely the results of the longitudinal, transversal, and Rayleigh velocities, Young modulus, transverse modulus and Poisson ratio of different bone porosity rates studied. Quantitative interpretation of the above results is utilized to evaluate the longitudinal velocity depending on the other physical parameters of bone. The obtained results show a direct effect of density, transverse velocity, Young's modulus and Poisson's ratio of the longitudinal wave velocity. Moreover, so far, there is no direct method to determine the mechanical properties of porous bone. That is why it seems useful to show the relationship between these properties. Correlations provide a better estimation of the physical properties of bones knowing the longitudinal velocity; this is deduced from the following simple mathematical relations:

$$V_t = 0.839V_l - 1258.577 \quad (15)$$
$$\rho = 0.406V_l + 390.089 \quad (16)$$
$$E = (0.406V_l^2 + 13330.049V_l + 11557873.854)10^3 \quad (17)$$
$$\nu = (-0.720V_l^2 - 4953.762V_l + 60543203.175)10^{-8} \quad (18)$$
$$G = (1.485V_l^2 - 5149.038V_l + 127552.145)10^3 \quad (19)$$

The data analysis indicates that the longitudinal velocity of ultrasound can be used to evaluate the elastic modulus of the porous material.

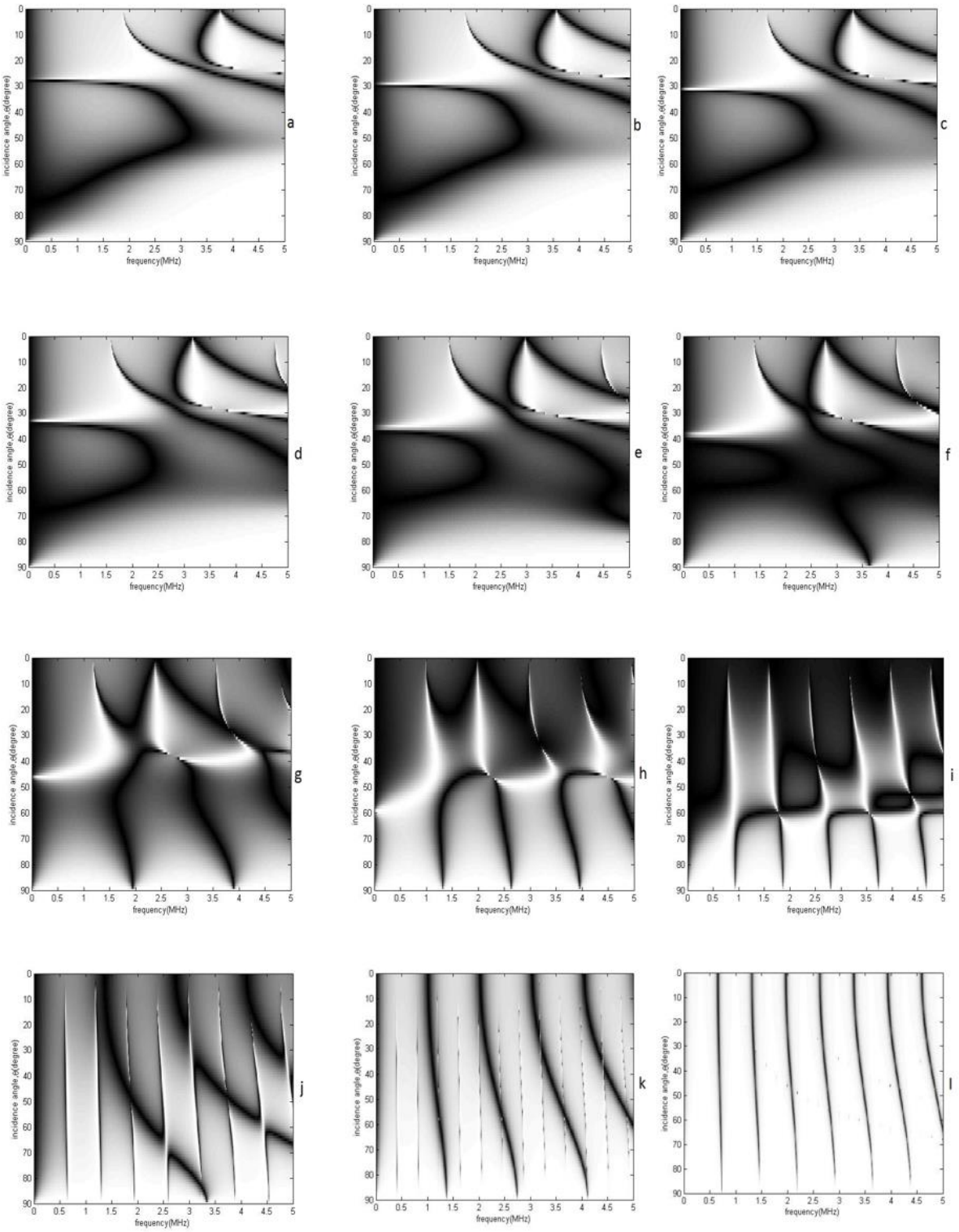

Fig. 5. Dispersion curves obtained theoretically for air-saturated trabecular bone plate for different porosity rates: a : 5%, b : 10%, c : 15%, d : 20%, e : 25%, f : 30%, g : 40%, h : 50%, i : 60%, j :70%, k: 80% and l : 90%.

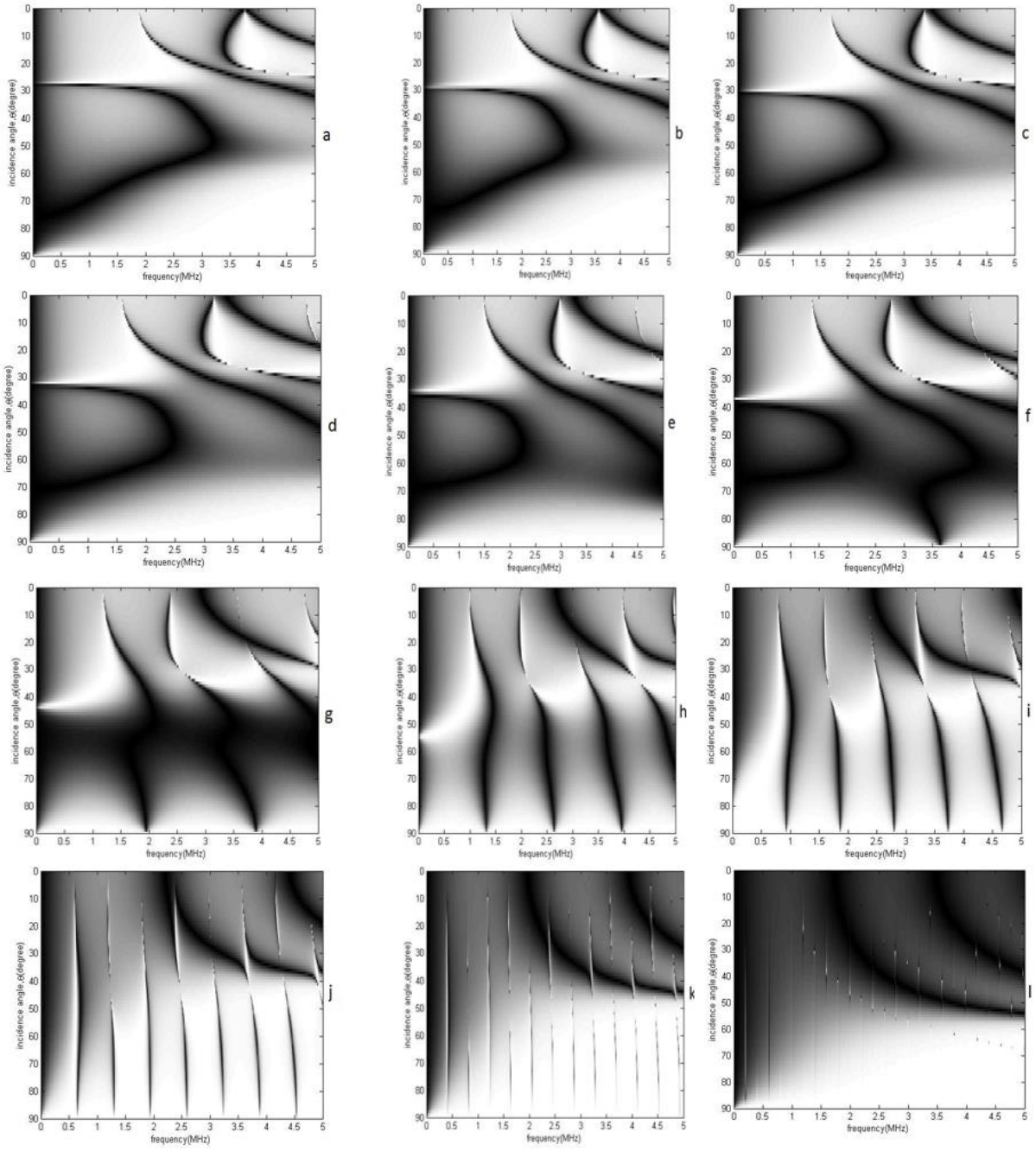

Fig. 6. Dispersion curves obtained theoretically for water-saturated trabecular bone plate for different porosity rates: a : 5%, b : 10%, c : 15%, d : 20%, e : 25%, f : 30%, g : 40%, h : 50%, i : 60%, j :70%, k: 80% and l : 90%.

Table 2. Values densities, acoustic wave velocities and elastic constants of water-saturated porous bone.

Porosity (%)	**ρ(Kg/m^3)**	**V_l(m/s)**	**V_t(m/s)**	**V_R(m/s)**	**E(GPa)**	**G(GPa)**	**ν(x10^{-3})**
0	1960	3861.0	1981.0	1850.8	20.32	7.69	321.3
5	1912	3743.0	1881,9	1760.8	18.02	6.77	330.8
10	1864	3624.9	1782,9	1670.6	15.88	5.92	340.4
15	1816	3506.9	1683,8	1580.1	13.90	5.19	350.2
20	1768	3388.8	1584,8	1489.3	12.07	4.44	360.0
25	1720	3270.8	1485,7	1389.3	10.40	3.79	370.0
30	1672	3152.7	1386,7	1307.0	8.87	3.21	380.1
40	1576	2916.6	1188.6	1123.6	6.23	2.22	400.4
50	1480	2680.5	990.5	938.8	4.12	1.45	420.9
60	1384	2444.4	792.4	735.1	2.50	0.86	441.3
70	1288	2208.3	594.3	566.2	1.33	0.45	461.0
80	1192	1972.2	396.2	378.3	0.55	0.18	479.0
90	1096	1736.0	198.1	189.5	0.12	0.04	493.4

3-2- Experimental results

3-2-1- Example of signals through the bone

Fig. 7 shows the incident signal generated by the transducer without sample(blue) and the signal transmitted by the plate of bovine trabecular bone (thickness =8 mm and porosity =50.8%)(red). Fig. 8 shows the incident signal generated by the transducer without sample (blue) and the signal transmitted by the plate of bovine trabecular bone (thickness =6.52 mm and porosity =60.4%)(red). These figures note that when the bone porosity increases the amplitude of the signals transmitted through the bone decreases. When the porosity of the bone increases, the bone becomes less dense and this is why we observe this reduction in the signal transmitted.

3-2-2- The ultrasonic measurements

It is hard or impossible to detect ultrasonic waves behind a whole bone as they are considerably attenuated by passing through the bone because of the high content of the air and wide intercellular gaps in the bone structure. Thus, the transmission method was used for measuring the high velocity within the bovine sample trabecular bone form of a parallelepiped plate. This non-destructive technique is fascinating to try the opportunity to assess the intrinsic quality of the bone by controlling its inner layer only knowing that the bone quality control starts from the trabecular part.

3-2-2-1- Masurement of ultrasonic velocity

For measuring the velocity of ultrasonic waves in the trabecular bone, we measure the flight time required for the wave to propagate the thickness thereof from which the ultrasonic signal that through by the bone. Thus the speed is calculated using the following formula:

$$V = \frac{d}{t_v} \tag{20}$$

where d is the thickness of the bone plate and t_v is the flight time.

3-2-2-2- Measurement of elastic properties

Some measurements were made on samples of bovine trabecular bone. Samples of the parallelepiped-shaped femur head of variable thickness and density (therefore variable porosity) were cut. After the soft tissue and bone marrow were removed from the bone samples, they were saturated by water.

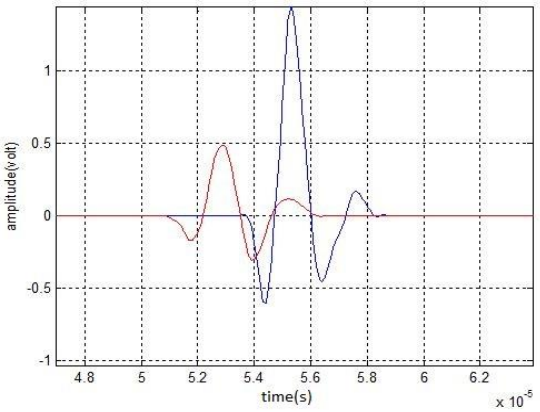

Fig. 7. Time signal for trabecular bone; thickness of the bone = 8 mm, porosity: 50.8%. Red: signal through the bone, Blue: signal through the water without bone.

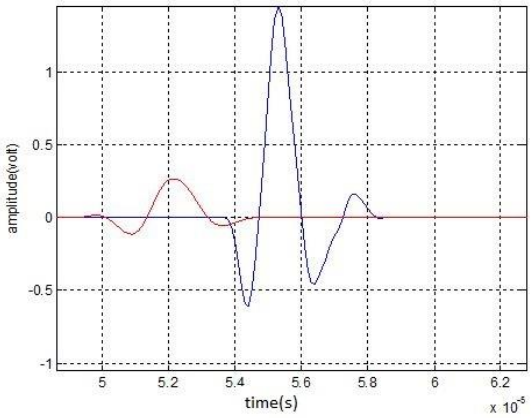

Fig. 8. Time signal for trabecular bone; thickness of the bone = 6.52 mm, porosity: 60.4%. Red: signal through the bone, Blue: signal through the water without bone.

In Table 3, we have listed the experimental ultrasonic velocities and elastic properties obtained on various samples as a function of bone porosity. This change is consistent with the theoretical values obtained using the Schoch model. The velocity decreases with increasing porosity. We measured the volume density, porosity, and the longitudinal speed of seven samples of trabecular bovine bone (Table 3). This work is only an introduction to the systematic study, already started to prepare a database of physical properties of trabecular, skeletal bones from different sites. Therefore, most of our discussion will focus on what we have seen so far. Nevertheless, even with the results we have obtained, we can draw some interesting conclusions limited to the samples studied.

The ultrasonic longitudinal speed is a primary parameter that provides information on some properties of trabecular bone (porosity and density). It is related to the fundamental properties of these bones. By observing the results shown in Table 3, we notice that the longitudinal speed varies from one sample to another. This variation is essentially due to the porosity. The analysis of our results shows that the sample with a low porosity has the highest longitudinal velocity. This finding is in good agreement with the behavior of many other porous materials [29]. This study confirms the sensitivity of the ultrasonic propagation velocity with variation in the bone porosity.

Table 3. Experimental values of densities, acoustic wave velocities and elastic constants of porous bones saturated by water.

Porosity(%)	**V_l(m/s)**	**ρ(Kg/m^3)**	**V_t(m/s)**	**E(GPa)**	**G(GPa)**	**ν**	**Relative Error**
50.8	2662	1472	974.9776	3.9808	1.3989	0.4225	9.0%
53.6	2522	1445	857.5104	2.9887	1.0420	0.4347	9.3%
59.8	2342	1385	706.4812	1.9401	0.6686	0.4499	7.3%
60.4	2285	1380	658.6552	1.6613	0.5704	0.4546	6.0%
70.1	2173	1287	564.6815	1.1879	0.4056	0.4638	8.3%
72.0	2151	1250	546.2224	1.1065	0.3776	0.4655	7.0%
73.2	2069	1257	477.4202	0.8368	0.2859	0.4721	7.0%

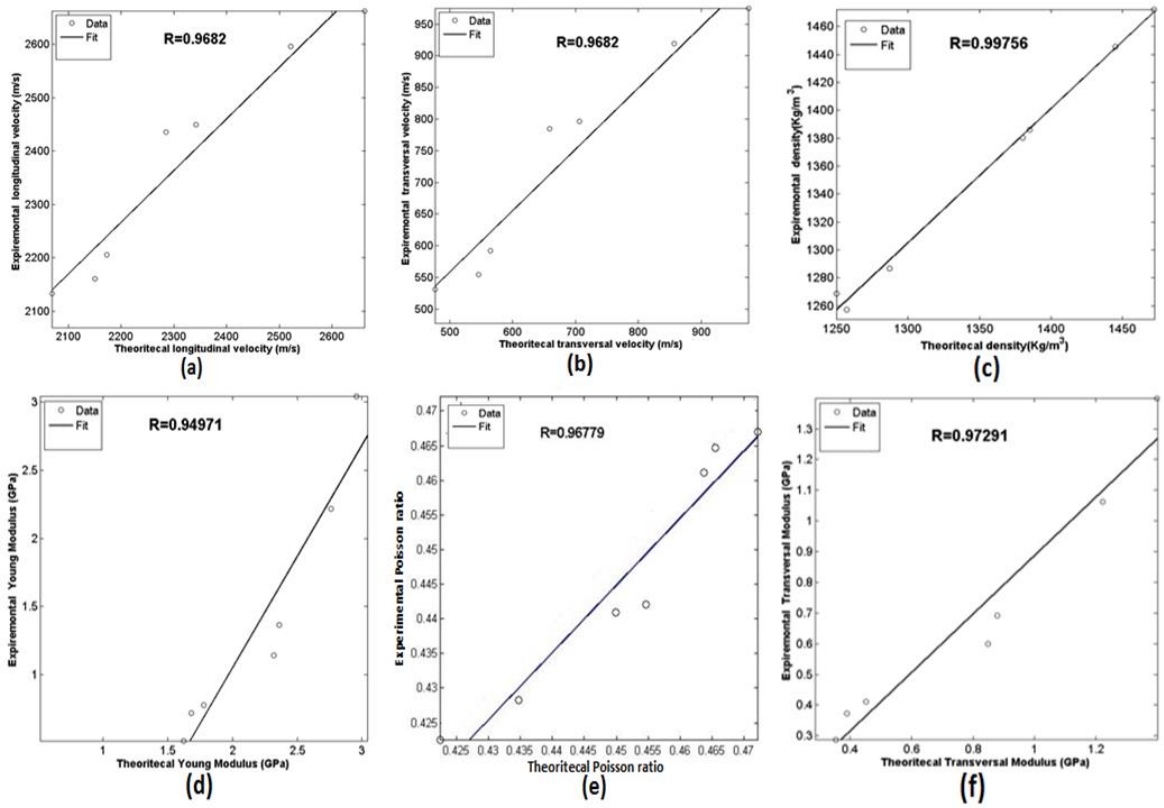

Fig. 9. Correlation between theoretical and experimental values of: a: longitudinal velocity, b: transversal velocity, c: density, d: Young modulus, e: Poisson ratio, f: transversal modulus.

The experimental data and theoretical predictions are similar, allowing us to conclude that the theory of propagation of Lamb waves is well suited to the description of the spread of the ultrasonic wave in the cancellous bone [30]. It also proves the validity Schoch model for the description of the wave Lamb propagation in cancellous bone.

3-3- Comparison between the theoretical values and the experimental values

We assume that these results may provide a reliable method to obtain a rapid characterization of bones; these results are also compatible with those found in the literature [9]. We found an excellent linear correlation between the porosity and in all other properties of the bone sample studied. Comparison of our theoretical results with those achieved experimentally demonstrates a good agreement, which constitutes a first step in validating our calculation program. The prediction appearance evaluated by using the following performance measures the correlation coefficient R. The corresponding definitions are given as follows [31]:

$$R_c = \frac{\sum_{i=1}^{n}(A_i - \bar{A})(P_i - \bar{P})}{\sqrt{\sum_{i=1}^{n}(A_i - \bar{A})^2 \sum_{i=1}^{n}(P_i - \bar{P})^2}} \quad (21)$$

where A is the theoretical value, P is the experimental value, $\bar{A}$ is the mean of the theoretical value, $\bar{P}$ is the mean of the experimental, and n is the total number of data.

Fig .9 shows the correlation between theoretical and experimental values of: longitudinal velocity (Fig 9-a), transversal velocity (Fig 9-b), density (Fig 9-c), Young modulus (Fig 9-d), Poisson ratio (Fig 9-e) and transversal modulus (Fig 9-f). The best results are obtained when the points are illustrated at the straight line. This means that the value of the correlation coefficient R is 1. The values of the correlation coefficient R between theoretical and experimental values are: R=0.99 for density, R=0.97 for transversal modulus, R=0.96 for longitudinal velocity, transversal velocity and Poisson ratio, and R=0.94 for Young modulus. Those values show that there is a positive and

almost perfect agreement between theoretical and experimental values of acoustics and elastics parameters.

4- Conclusion

In this article, two complementary approaches to ultrasonic characterization of porous bones were proposed and realized. At first, we used the Schoch theory as a model of the Lamb wave propagation in porous bone. Second, we evaluated an experimental study of the porous bone elastic proprieties from the wave longitudinal transmitted in the bovine cancellous bone sample. Experimental validation of this model using waves transmitted through samples of bovine cancellous bone was performed and an excellent agreement was found between theory and experiment. So, from these mechanical properties of cancellous bone we can know that is normal or osteoporotic bone.

We conclude that the Schoch theory is adequate for the propagation of Lamb wave in cancellous bone to the effect that further review is necessary to explain all the observed phenomena. We also think that our research could have interesting applications in the diagnosis of other diseases or traumas of bones and even other tissues and vital organs, and in the characterization of non-living materials /structures, natural or fabricated.

References

[1] Langton C.M. Njeh C.F, The Physical Measurement of Bone, IOP, Bristol, 2004.

[2] D. Ahite, Contribution to the development of an ultrasonic device for characterizing the cortical bone by Lamb waves, Ph.D. Thesis at the University of Valenciennes and Hainaut Cambresis, Valenciennes, 2000.

[3] Foldes A.J. et al., "Quantitative ultrasound of the tibia: a novel approach for assessment of bone status". Bone, Vol. 17, 1995, pp. 363-367.

[4] Lee, K. I., and Suk Wang Yoon. "Feasibility of bone assessment with leaky Lamb waves in bone phantoms and a bovine tibia", The Journal of the Acoustical Society of America 115.6, 2004, pp. 3210-3217.

[5] G. Lowet and G. Van der Perre, "Ultrasound velocity measurement in long bones: measurement method and simulation of ultrasound wave propagation", J. Biomech., Vol. 29, 1996, pp. 1255-1262.

[6] M. Muller, P. Moilanen et al., "Comparison of three ultrasonic axial transmission methods for bone assessment", Ultrasound Med. Biol., Vol. 31, 2005, pp. 633-642.

[7] A. Tatarinov, N. Sarvazyan, A. Sarvazyan, "Use of multiple acoustic wave modes for assessment of long bones: model study", Ultrasonic, Vol, 43, 2005, pp. 672-680.

[8] V.C. Protopappas, D.I. Fotiadis, K.N. Malizos, "Guided ultrasound wave propagation in intact and healing long bones", Ultrasound Med. Biol., Vol. 32, 2006, pp. 693-708.

[9] Pascal Laugie: Bone Quantitative Ultrasound. Guillaume Haat Editors, 2011.

[10] Abiddine Zine El Fellah, Acoustic propagation in heterogeneous porous media, Ph.D. thesis, CR1 at LMA, CNRS Marseille, 2010.

[11] Sylvain BERGER, Contribution to the characterization of porous media by acoustic methods: estimation of physical parameters, Ph.D. Thesis, Graduate School of the University of Maine, 2004.

[12] E.A. Holland and L.F. Rogers, "Osteoporosis: Impact on the elderly, societal concerns, and the role of radiology", Curr. Probl. Diagn. Radiol., Vol. 18, NO. 2., 1989, pp. 41 - 61.

[13] Schoch A, "Sound transmission through plates", Acoustica, Vol. 2, 1952, pp. 1-17.

[14] Brekhovskikh L M, Waves in Layered Media, 2nd edn New York: Academic Press, 1980, p 503.

[15] R. J. M. Da Fonseca and J. Attal, Elastic micro-characterization of porous materials by acoustic signature, Ph.D. Thesis, University of Montpellier II, 1995.

[16] R. J. M. Da Fonseca, "Acoustic investigation of porous silicon layers", J. Mater. Sci., Vol. 30, 1995, pp. 35-39.

[17] R. J. M. Da Fonseca, "Acoustic microscopy investigation of porous silicon", Thin Solid Films, Vol. 255, 1995, pp. 155-158

[18] K. K. Phani, A.K.Maitra, "Strength and elastic modulus of a porous brittle solid: an acousto-ultrasonic study", J. Mater. Sci., Vol. 29, 1986, pp. 4335-4341.

[19] K. K. Phani, A.K. Maitra, "ultrasonic evaluation of elastic parameters of sintered

powder Compacts", J. Mater. Sci., Vol. 29, 1994, pp.4415-4419.
[20] I. A. Victorov, "Rayleigh and Lamb waves: physical theory and applications. Ed. Plenum Press, New York, 1967.
[21] Hosokawa A., Otani T., "Ultrasonic wave propagation in bovine cancellous bone", Journal of the Acoustical Society of America, Vol. 101, 1997, pp. 558-562.
[22] A. Hosokawa, "Simulation of ultrasound propagation through bovine cancellous bone using elastic and Biot's finite-difference time domain method", Journal of the Acoustical Society of America, Vol. 118, 2005, pp. 1782-1789.
[23] A. Hosokawa, "Numerical analysis of variability in ultrasound propagation properties induced by trabecular microstructure in cancellous bone", IEEE Transactions on Ultrasonics Ferro electrics and Frequency Control, Vol. 56, 2009, pp. 738-747.
[24] Hosokawa A., "Effect of porosity distribution in the propagation directionon ultrasound waves through cancellous bone", IEEE Transactions on Ultrasonic Ferro electrics and Frequency Control, Vol. l57, 2010, pp. 1320-1328.
[25] O. Diligent , Interaction between fundamental Lamb modes and defects in plates. PhD Thesis, Imperial College London: London, UK, 2003.
[26] D. Abassi, Contribution to the non-destructive characterization of terrestrial and extraterrestrial rocks by ultrasound techniques, Ph.D. Thesis, IBN ZOHR University, Morocco, 2014.
[27] L. Scandelari, Generation and detection of Lamb waves with the help of P (VF2- VF3): application to liquid density measurement, Ph.D. Thesis, Joseph-Fourier University, Grenoble, 1999.
[28] G. Haiat, F. Padilla, "Relationship between ultrasonic parameters and apparent trabecular bone elastic modulus: A numerical approach", Journal of Biomechanics, Vol. 42, 2009, pp. 2033-2039.
[29] G. Mavko , T. Mukerji, and J. Dvorkin. The rock physics handbook: Tools for seismic analysis of porous media, Cambridge University press, 2009.
[30] Y. Nagatani, K. Mizuno, "Numerical and experimental study on the wave attenuation in bone FDTD simulation of ultrasound propagation in cancellous bone", Ultrasonics, Vol. 48, 2008, pp. 607-610.
[31] L. Haifan, and J. Wang. "Integrating independent component analysis and principal component analysis with neural network to predict Chinese stock market", Mathematical Problems in Engineering, 2011.